Article

Enhanced surface interaction of water confined in hierarchical porous polymers induced by hydrogen bonding.

Emilia V. Silletta, Manuel Isaac Velasco, Cesar G. Gomez, Miriam C. Strumia, Siegfried Stapf, Carlos Mattea, Gustavo Alberto Monti, and Rodolfo H. Acosta

Langmuir, **Just Accepted Manuscript** • DOI: 10.1021/acs.langmuir.6b00824 • Publication Date (Web): 24 Jun 2016

Enhanced surface interaction of water confined in hierarchical porous polymers induced by hydrogen bonding.

Emilia V. Silletta[1], Manuel I. Velasco[1], Cesar G. Gomez[2], Miriam C. Strumia[2], Siegfried Stapf[3], Carlos Mattea[3], Gustavo A. Monti[1] and Rodolfo H. Acosta[1].*

[1]FaMAF-Universidad Nacional de Córdoba and IFEG-CONICET, 5016 Córdoba, Argentina.

[2] Departamento de Química Orgánica, Facultad de Ciencias Químicas (IMBIV-CONICET), Universidad Nacional de Córdoba, Haya de la Torre y Medina Allende, Edificio de Ciencias II - Ciudad Universitaria, 5000 Córdoba, Argentina.

[3]FachgebietTechnischePhysik II / Polymerphysik, Institute of Physics, TechnischeUniversitätIlmenau, PO Box 100 565, 98684 Ilmenau, Germany

ABSTRACT: Hierarchical porous polymer systems are increasingly applied to catalysis, bioengineering or separation technology due to the versatility provided by the connection of mesopores with percolating macroporous structures. Nuclear magnetic resonance (NMR) is a suitable technique for the study of such systems as it can detect signals stemming from the confined liquid and translate this information into pore size, molecular mobility and liquid-surface interactions. We focus on the properties of water confined in macroporous polymers of ethylene glycol dimethacrylate and 2-hydroxyethyl methacrylate [poly(EGDMA-co-HEMA)] with different amounts of cross-linker, in which a substantial variation of hydroxyl groups is achieved. As soft polymer scaffold may swell upon saturation with determined liquids, the use of NMR is particularly important as it measures the system in its operational state. This study combines different NMR techniques to obtain information on surface interactions of water with hydrophilic polymer chains. A transition from a surface induced relaxation in which relaxivity depends on the pore size to a regime where the organic pore surface strongly restricts water diffusion is observed. Surface affinities are defined through the molecular residence times near the network surface.

1. INTRODUCTION

The transport properties of fluids imbibed in a porous media play a key role in several research areas, and determine the efficiency of processes such as catalysis[1, 2, 3] separation,[4, 5] energy[6] and bioengineering.[7, 8] Determination of accurate morphological features of porous media is a current challenge to material scientists, as many properties of stationary supports depend not only on the void sizes distribution but also on their connectivity and liquid surface interactions. Porous polymeric scaffolds have a wide range of applications and can be prepared with a controlled hierarchy of micro-, meso-, and macroporous spatial domains.[9, 10, 11, 12] Because of the hydrophilic characteristic of these materials, water not only diffuses into pore structures, but also swells the network developing a layer of gel inside the material. A gel phase usually exhibits a better performance in terms of accessibility to specific active sites on the surface,[13] however its mechanical properties hinder the span of possible applications. The possibility to generate porous polymers with a gel fraction thus enhances the material performance by combining the gel properties with the great surface to volume ratio provided by the porous structure.

As the properties of a functional composite depend on a multitude of processes, which occur over a wide spectrum of length and time scales, complementary use of different techniques may be required for a comprehensive characterization. Indirect methods, as nitrogen absorption, mercury porosimetry, small angle X-ray, or neutron scattering, provide average information, while imaging methods provide a direct measure of microstructural properties.[14] In particular 3D focused ion beam scanning electron microscopy (FIB-SEM) has been successfully applied to porous polymers with high imaging resolution.[15, 16] These methods provide information of the dry state and may additionally affect the pore structure, for instance, mercury intrusion relies on monitoring changes in pressure as the system is flooded which may induce changes in the morphology for soft polymers. Additionally, when the porous media is saturated with a fluid which is able to swell the polymer, changes in the porosity can be expected.[10]

Nuclear magnetic resonance (NMR) is a suitable technique for the study of molecular dynamics of different liquids confined in porous matrices. Several methods based on monitoring the restricted diffusion of liquid molecules confined in a porous matrix, and their relaxation properties render information of void size, pore interconnectivity and liquid-surface interactions.[17, 18, 19] For liquids contained in a pore, it is expected that two contributions are present, a layer that strongly interacts with the surface and a more mobile fraction. This effect has been quantified for a water interacting with a variety of inorganic porous systems in the nanoscale range, nanoparticles and biomolecules, [20, 21] and experimentally shown for confined water or ionic liquids.[22, 23, 24] NMR relaxation times measurements have been widely used to study molecular dynamics of liquids imbibed in porous media. Brownstein and Tarr[25, 26] have demonstrated that the longitudinal (T_1) and transversal (T_2) relaxation times characterize the pores since they are proportional to the surface to volume (S/V) ratio. Considering that the decay of the magnetization is due to diffusion, the relaxation time corresponds to the time taken to migrate across the pore, where each spin that encounters the wall is lost by relaxation.[17] Relaxation is given by two factors, the S/V and surface relaxivity parameter ρ: $T_i^{-1} = \rho_i \, S/V$, with i=1,2. If the system dimension is known, the relaxation times

may be used to infer liquid-surface properties through the determination of ρ_i. In order to combine this information, it is desirable to determine the pore size in the same conditions as the relaxation measurements are carried out. A powerful non-invasive approach to determine void sizes by NMR was introduced by Song et al.[27] It relies on the fact that small distortions in the magnetic field appear within a heterogeneous sample due to variations in the local magnetic field susceptibilities between the solid matrix and the confined liquid. A signal loss is produced as a liquid molecule diffuses through these internal magnetic field gradients, which can be readily used to obtain information on the pore dimension. This experiment is referred to as DDIF (Decay due to Diffusion in the Internal Field).[27, 28, 29] A combination of DDIF with frequency dependent T_1 measurements has been applied to study surface relaxivity in porous ceramics[30] and in combination with T_2 in rock cores with different lithologies at low magnetic fields.[31]

Relaxation times may additionally be affected by the interaction of the fluid with the porous matrix, where the interplay of surface relaxation and pore structure is governed by the fluids' molecular dynamics. Fast Field Cycling (FFC) relaxometry[32] has proven to be an ideal tool to extract this information in a wide range of characteristic times, where fluctuations of the spin interactions with correlation times up to eight orders of magnitude greater than those of the bulk liquid are found. When a molecule adsorbs from solution to the wall surface, it adopts preferential orientations relative to the local pore surface. Once a molecule desorbs it may diffuse into the bulk; however, under strong adsorbing conditions it may be reabsorbed, experiencing a flight close to the surface. This relaxation mechanism is known as reorientations mediated by translational displacements (RMTD)[33] and has been applied, for instance, to describe molecular displacements of helicogenic peptides on hydrophilic fused silica surfaces using single molecule fluorescence microscopy.[34] Besides probing the surface topology by molecular reorientations, a molecule diffusing near the pore wall surface may interact with specific sites that induce an additional relaxation mechanism. For paramagnetic sites a model that takes into account the molecular surface residence time and the interval in which a molecule encounters a relaxation site was introduced by Korb et al.[35, 36] This model has been successfully applied for the study of catalysts surface interactions with different liquids.[37]

Applications of these NMR techniques, either stand alone or combined, are used in different research fields mainly in inorganic matrices such as those found in the oil industry,[38, 39] cement paste research,[40, 41] study of soil permeability[42] and in the field of catalysis.[37] However, there is a surprisingly low amount of researches on NMR applied to organic porous systems. In this work we study liquid-surface interactions for water confined in a porous polymeric system, which is composed by macroporous polymer beads that can develop a permanent porous structure even in the dry state. We combine different NMR techniques to study the behavior of confined water. The distribution of pore size determined with the DDIF sequence, combined with relaxation measurements indicates that surface relaxation follows the theory proposed by Brownstein and Tarr in the entire porous network, except for water in close contact with the polymer mesh. In this case, strong interactions with superficial hydroxyl groups render RMTD. With the aid of frequency dependent experiments, the characteristic molecular hopping and

residence times at the pore surface are obtained. We observe that the surface residence times greatly increase when the networks swell, developing a gel fraction.

2. MATERIALS AND METHODS

2.1 Porous Polymeric Networks. Polymer beads with hierarchical pore structure of ethylene glycol dimethacrylate and 2-hydroxyethyl methacrylate [poly(EGDMA-co-HEMA)] were synthesized as previously described.[43] In order to obtain 10 g of dry polymer, 3 mol (6.2 mL) of HEMA, 1 mol (3.2 mL) of the cross-linker EGDMA and 9.3 mol (17 mL) of porogenic agent cyclohexane were stirred at 85ºC in 77 mL of water. Benzoyl peroxide (BPO), Riedel de Häen-Germany, (0.411 g, 2.44 mol%) was added as free-radical initiator and poly(vinyl pyrrolidone)(PVP), Kollidone 90, Fluka-Switzerland, was used as suspension stabilizer. Different polymeric networks were obtained varying the cross-linker content of 6, 10, 17, 25 and 33 mol% of EGDMA. The resulting polymer beads were washed with distilled water and afterwards with ethanol. Samples were then dried in an oven at 70 °C, at ambient pressure, until constant mass was reached.

The resulting system consists of polymer beads that contain large agglomerates of microspheres (100 - 200 nm) as shown in Scheme 1.[10, 44] Each microsphere consists in turn of smaller nuclei (10 - 20 nm) which are nonporous and represent the most highly cross-linked regions of the system. The nuclei are blended to some extent, leaving an inter-space which is mainly responsible for the great surface to volume ratio of this type of material. The cavities between the microspheres render a second type of intermediate void. Finally, larger pores are generated when the microspheres are agglomerated into larger irregular entities in the polymer material. Since the proportion of used monomer affects the matrix polarity, the interaction of water with different polymer systems is expected to change together with the amount of cross-linker. HEMA has a hydroxyl and ester functional group, while EGDMA only an ester group. Both monomers are able to form hydrogen bonds with water molecules through the carbonyl or hydroxyl group, but only HEMA can act as hydrogen donor. Since the total amount of monomers is constant for all networks, an increase in cross-linker implies that the content of HEMA or hydroxyl groups in the polymer network decreases (see Scheme 1). Consequently the hydrophilicity of the matrix is modified from a more hydrophilic (6 mol % of cross-linker) to a less hydrophilic one (33 mol % of cross-linker).

2.2 NMR Experiments. Small samples of polymer beads were immersed in a vial containing distilled water at room temperature for 24 h in order to reach the full swelling of the network. Samples of 75 mg weight were extracted from the vial and gently placed in a 5 mm outer diameter NMR sample holder and sealed to avoid evaporation. Each sample was prepared five times and measured in independent experiments. All experiments were carried out at 30 ºC and ambient pressure. Pore size determination and 2D relaxation maps were acquired with a Magritek Kea2 spectrometer operating at 60 MHz for protons. A 1.4 T permanent magnet (Varian EM 360) equipped with a homemade probe was used. In the DDIF sequence the encoding time was set to t_e= 0.5 ms and t_D ranged from 0.5 ms to 4 s in 32 logarithmically increased steps. $D = 2.6\times10^{-9}$ m^2/s for bulk water was consid-

ered.[45] For the T_1-T_2 maps, T_1 was encoded in the indirect dimension with an inversion-recovery sequence in 50 time steps and T_2 with the multipulse Carr-Purcell-Meiboom-Gill (CPMG) pulse sequence, where the echo-time (t_E = 0.5 ms) is set short enough to mitigate diffusion effects, and the acquisition of 6000 echoes. Fast Field Cycling experiments were carried out in a Stelar Spinmaster FFC2000 1T C/DC relaxometer at 30ºC with frequencies ranging from 0.01 to 20 MHz. Data corresponding to 60 MHz and 300 MHz were included in the relaxation profiles. The latter were acquired with a Bruker Avance II console using a DOTY DSI-703 proton dedicated probe with proton background signal reduction. Diffusion measurements were carried out with a PM5 NMR-MOUSE from Magritek GmbH, with a static magnetic field gradient of 23.5 T/m using a stimulated echo pulse sequence, with a diffusion time of Δ = 1 ms.

3. RESULTS AND DISCUSSION

3.1 Pore Size Characterization. Pore size distributions (PSD) were obtained by using the DDIF sequence. This sequence relies on the acquisition of a stimulated echo; where a short encoding period t_e is used to map the local gradient fields, followed by a diffusion period t_D in which diffusion through the internal fields takes place.[27, 28] The decay on the echo intensity as a function of t_D is compared to a reference signal, which monitors relaxation due to T_1. For a detailed description of the method see ref.[29] Subtraction of both signals renders a data set with a characteristic decay time τ that is related to the pore diameter by the following expression: $d = \pi\sqrt{D\tau}$; where D is the diffusion coefficient of bulk water and the pores are assumed to have a spherical shape. When a distribution of pore size is present, different τ values can be extracted from the signal decay by application of an Inverse Laplace Transformation (ILT) algorithm. Typical accessible pore sizes that can be probed with water at room temperature are in the order of 1 μm - 500 μm. For the highly cross-linked polymer networks three distinct void dimensions are observed. Large pores (P_1) correspond to void spaces between agglomerated microspheres, with a mean diameter of 90 μm (see Fig. 1). A second pore size (P_2) of 35 μm is assigned to the inter-space between the microspheres, and a third population (P3), with an apparent diameter of 10 μm. The determination of this last cavity size corresponds to signals arising from water in close contact with the polymer chains, via hydrogen bonds with surface OH groups, and probably a layer of structured water also contributes to this signal. Previous experiments have shown that this type of water does not evaporate from the system at ambient temperature and pressure.[46] As the amount of cross-linker is reduced the system increases its ability to swell. This leads to a change in the size distribution of the polymer beads, which affects the overall pore size distribution. The change in the overall porosity of the system was reported by means of gravimetric experiments[10] as well as the changes in the individual T_2 values for water contained in each pore.[46, 47] A maximum in the diameter of P_2 is observed for 17 mol % of EGDMA content. For lower cross-linker content, the primary particles suffer deformations rendering a collapse in the pore structure. This is evidenced by the decrease in pore size of P_2 as well as the presence of large pores (Ps) of around 70 μm, which are assigned to water contained in the swollen polymer matrix, where a gel phase is developed. The values of P_1 present a large dispersion as these are susceptible to the packing condition in

the NMR sample holder. A representative curve of the PSD for networks with 33 mol % of EGDMA content is shown in Fig. 1b. The relative amount of water in the different cavities for networks prepared with 33 mol % of EGDMA content was determined to be of 60 % for pores P_1; more than 35 % for pores P_2 and c.a. 5 % for water corresponding to population P_3. Similar values were obtained for all samples.

3.2 Surface Relaxation. Surface relaxation is in general investigated by inspection of the T_1/T_2 ratio, as this parameter is sensitive to molecular dynamics. T_1 and T_2 have different dependencies on rotational and translational motions, consequently, the ratio T_1/T_2 is considered to be analogous to the energy of adsorption on a surface or the surface interaction strength.[48] Relaxation rates are dependent on the magnetic field, in particular at high fields a collapse into a single T_1 relaxation value is observed for the contribution of water confined in all pores, as shown in Fig. S1. When molecules are adsorbed on surfaces their rotational and diffusional dynamics are modified, rendering an increase in the T_1/T_2 value.[36] Two independent experiments that determine each relaxation time may be carried out, however, it has been shown that a two dimensional experiment that encodes longitudinal relaxation, while detecting transverse relaxation renders a higher level of information.[49]

Figure 2a shows a T_1-T_2 correlation map obtained at 60 MHz for a sample prepared with 33 mol % of EGDMA content. Water in P_1 presents a ratio $T_1/T_2 = 5.4$, while in P_2 $T_1/T_2 = 13.5$ and 25 in P_3. The change in the T_1/T_2 ratio for different pore sizes could be attributed in principle to the influence of the internal field gradients in the determination of T_2; however, this effect was observed to be minimal for the short selected echo times. This behavior was supported by performing several measurements as a function of the echo time (data not shown). This indicates that different surface interactions for liquids confined in each cavity are present, even though the synthesis process ensures an homogeneous distribution of monomeric units throughout the sample. In homogeneous systems, as for instance in Indiana rocks saturated with water, distributions parallel to the $T_1 = T_2$ line are observed, indicating that a single surface relaxation mechanism is present throughout the system and that relaxation is due only to a local S/V variation.[49] Additionally, the value of T_1/T_2 ratio for different pores is greater as the cross-linker content is decreased, where a striking increase is observed for P_3, ranging from 25 to 123, as shown in Fig. 2b. For water contained in the remainder of the cavities, an inverse dependence with the pore size is exhibited.

Assuming a distribution of spherical pores, the relaxation times can be expressed as: $T_i^{-1} = 6\rho_i/d$ if relaxation arises solely from a reduction of molecular reorientations. This gives rise to a linear behavior of the relaxation rates with respect to the inverse of the cavity size, as shown in Fig. 3a for longitudinal relaxation of water contained in all cavities of the different samples.

The longitudinal surface relaxivity is obtained from the slope giving rise to a constant average value of $\rho_1 = (0.020 \pm 0.001)$ mm/s, that is, at 60 MHz T_1 relaxation of confined water is a surface-limited process in the whole system environment. The same behavior is observed for transverse relaxation in P_1, P_2 and P_s, with an

average relaxivity of $\rho_2 = (0.20 \pm 0.04)$ mm/s. NMR relaxation rates of water corresponding to population P_3 does not depend on the cavity size for networks prepared with high cross-linker content (33, 25 and 17 % of EGDMA), and changes when samples develop a gel fraction (6 and 10 mol% of EGDMA content) as shown in Fig. 3b.

The question that arises is if the pore size determined by DDIF for P3 is a real void size or we are in the presence of a limitation of this particular technique. It must be kept in mind that in order to determine the PSD with the DDIF sequence, the molecular displacements should cover the whole pore space, thus acquiring information of the internal gradient distributions on the phase of the NMR signal. For water corresponding to P3 an apparent diffusion coefficient $D_a = 0.2$ m^2/s was found, while for larger cavities $D_a = 1.8$ m^2/s. For the short diffusion time used (Δ = 1 ms) the mean square displacement is given by the diffusion length: $l_D = \sqrt{D\Delta} = 1.6\ \mu$m, however this displacement does not account for the large differences in the apparent diffusion coefficients for the PSD shown in Fig. 1a. This data, together with the transverse relaxation times imply that P3 must be interpreted as a fraction of water in strong interaction with the polymeric pendant chains. These structures configure a zone where water diffusion is strongly restricted as shown in Scheme 2, this behavior is typical when dealing with organic systems, where transverse relaxation gives a measure of the direct interaction of water molecules with the polymeric matrix.[50] In summary, the systems under study can be treated as hierarchical distributed pores, formed by a hydrated polymer matrix. Information on the interaction of water with this surface is highly relevant for the design of specific applications. In the next section we focus on this particular aspect.

3.3 Bound Water Relaxation Dispersion. The residence time of a molecule on a pore wall surface is characterized by surface correlation times that can potentially be determined by FFC relaxation experiments. The basic FFC relaxometry experiment consists of three steps. Initially the spin system is polarized at high field until the nuclear magnetization reaches its saturation. Subsequently, the magnetic field is switched to a value B_r for a variable time t_r, during which the magnetization relaxes towards its new equilibrium value. A final magnetic field step, in which the magnetic field is switched to the intensity at which detection of the NMR signal is performed, is carried out. Magnetization is detected with a 90° rf pulse.[32] At each B_r magnetic field the magnetization shows a multi-exponential decay, and the relaxation time distribution can then be obtained by application of an ILT algorithm to discriminate the different environments (see Fig. S1). The relaxation rates as a function of the Larmor frequency for hydration water (P_3) are shown in Fig. 4 for samples with a 6 and 33 mol % of EGDMA content. When the liquid molecules are adsorbed on the pores wall surface, the spin-lattice relaxation rate T_1^{-1} measured at relatively low magnetic fields is sensitive to the slow reorientational process of the molecules on the topology of the surface. Such reorientations are modulated by translational degrees of freedom, and give rise to RMTD,[19] while water contained in the larger voids does not show this behavior. RMTD has also been recently used to describe solvent dynamics in supramolecular gels.[51, 52]

In the case of normal diffusion, the probability density for a molecular displacement in a given time has a Gaussian form, and can be described in terms of modes with wavenumbers *k.* When every reorientational autocorrelation function for the *k*-diffusive mode decays exponentially, it can be represented with a characteristic time $\tau_k = (Dk^2)^{-1}$. The spectral density can be considered as a linear combination of Lorentzian-type contributions of all *k*-diffusive modes between k_{min} and k_{max}, weighted by the orientational structure factor $P(k)$,[53]

$$f_{k,RMTD}(\omega) = \int_{k_{min}}^{k_{max}} P(k) \frac{2\tau_k}{1+(\tau_k\omega)^2} dk.$$

Assuming that in the range between k_{min} and k_{max} all modes are equally weighted, the relaxation rate induced by RMTD is given by

$$T_1^{-1}(\omega) = A_{\mathrm{RMTD}} \left\{ \frac{1}{\omega^{\frac{1}{2}}} \left[f\left(\frac{\omega_{max}}{\omega}\right) - f\left(\frac{\omega_{min}}{\omega}\right) \right] + \frac{4}{(2\omega)^{\frac{1}{2}}} \left[f\left(\frac{\omega_{max}}{2\omega}\right) - f\left(\frac{\omega_{min}}{2\omega}\right) \right] \right\},$$

with $f(x) = \arctan\left(\sqrt{2x}+1\right) + \arctan\left(\sqrt{2x}-1\right) - \mathrm{artanh}\left(\frac{\sqrt{2x}}{x+1}\right)$ and $\omega_{min,max} = 2\pi/\tau_{k_{max,min}}$. The pre-factor A_{RMTD} depends on the residual dipole-dipole proton interactions, which are averaged by local molecular reorientations, and on the diffusion coefficient. The RMTD model considers that a molecule has a short surface residence time, but returns frequently to the surface, maintaining its orientation relative to the surface and then its orientational memory, which is lost by diffusion along a curved surface.

The maximum correlation time $\tau_{k_{max}}$ is associated to the time in which a molecule completely loses its contact with the surface, and diffuses into the liquid bulk, that is, it represents a surface residence time. From the fittings shown in Fig. 4, $\tau_{k_{max}} = 3.0$ μs and $\tau_{k_{max}} = 1.3$ μs are obtained for networks with 6 and 33 mol % of EGDMA content respectively. The time a molecule spends near the surface with a characteristic orientation given by its topology, is two times greater for networks with a lower amount of cross-linker (high degree of surface OH groups), compared to the most cross-linked ones (which have the smallest concentration of surface OH groups).

On the other hand, $\tau_{k_{min}}$ represents the rate of water molecular jumps between hydroxyl groups of HEMA contained on pore wall surface, which occur during the residence time. The obtained values are: $\tau_{k_{min}} = 1.3$ ns and $\tau_{k_{min}} = 2.0$ ns for networks with 6 and 33 mol % of EGDMA content respectively. Here it can be observed that the time between molecular jumps increases as the amount of surface OH groups is lower (highly cross-linked sample). Using the Einstein-Smoluchowski relation for a two-dimensional movement with the apparent diffusion constant, $\langle r \rangle^2 = 4D_a\tau$, mean displacements in the order of 1 nm are obtained, indicating the distance of OH groups that interact with water molecules. It should be noted that a water molecule probably does not meet all OH groups on the surface during the experimental time, and that the jumps are not necessarily between adjacent OH groups. The long molecular residence time in diffusion restricted zone (see Scheme 2) enables the existence of a

dispersion of the RMTD type, while in inorganic matrices this relaxation mechanism is observed for pores in the range of the nanometers.

In analogy with the model used by Godefroy and co-workers,[36] we define a measure of the surface affinity as the ratio $S_a = \tau_{k_{max}}/\tau_{k_{min}}$,[36] which represents the number of water molecular jumps during the surface residence before total desorption. For networks with a lower cross-linker content and a larger amount of surface OH groups $S_a = 2300$; while for 33 mol % of EGDMA, $S_a = 650$. The percentage change between the surface affinities of water in both types of networks is 71 % due to the variation of surface OH groups, while the percentage variation of the T_1/T_2 ratio is 79%, supporting previous observations that at intermediate fields this ratio is a measure of surface interaction strength.

4. CONCLUSIONS

We have shown that by combining different NMR techniques, the PSD of hierarchical porous polymers as well as the water surface affinities can be described in detail. For the systems used in this work, we determined that as the percentage of cross-linker decreases, surface interaction of water is enhanced due to the increase pendant HEMA groups, which increase the amount of hydroxyl groups in the surface. The development of tunable systems in terms of pore size distributions and interactions at molecular level broaden the spectra of applications of porous organic materials. In this regard, the ability to control the development of a gel phase and the amount of surface hydroxyl groups may prove very useful in the chemical design of materials with a desired specific surface-liquid interaction. This has applications for instance in HPLC systems with an extended performance, liquid separation, or in the specification of catalytic or enzymatic reactions. The persistence of these properties upon external stress, such as that given by a flowing liquid is subject of ongoing research. We envision that the approach presented in this work will be important to discern surface interactions in organic porous scaffolds, which may be used to enhance the performance of this type of materials for a special application.

AUTHOR INFORMATION

Corresponding Author

*racosta@famaf.unc.edu.ar

Author Contributions

The manuscript was written through contributions of all authors. / All authors have given approval to the final version of the manuscript.

ACKNOWLEDGMENTS

Authors thank F. Vaca Chávez for helpful discussions and Petrik Galvosas from Victoria University of Wellington, New Zealand, for providing us with the 2D inverse Laplace transformation software. We would like to

acknowledge the financial support received from CONICET, ANPCYT and SeCyT-UNC. M.I. Velasco thanks DAAD for the traveling fellowship.

REFERENCES

1. Islam, S. M.; Tuhina, K.; Mubarak, M.; Mondal, P. Hydrogenation of various organic substrates using polystyrene anchored orthometallated ruthenium (II) complex as catalyst. *J. Mol. Catal. A-Chem.* **2009,** *297* (1), 18-25.

2. Abu-Elfotoh, A. M.; Tsuzuki, K.; Nguyen, T. B.; Chanthamath, S.; Shibatomi, K.; Iwasa, S. Quinones synthesis via hydrogen peroxide oxidation of dihydroxy arenes catalyzed by homogeneous and macroporous-polymer-supported ruthenium catalysts. *Tetrahedron* **2013,** *69* (40), 8612-8617.

3. Wu, C.-D.; Hu, A.; Zhang, L.; Lin, W. A Homochiral Porous Metal−Organic Framework for Highly Enantioselective Heterogeneous Asymmetric Catalysis. *J. Am. Chem. Soc.* **2005,** *127* (25), 8940-8941.

4. Gölgelioğlu, Ç.; Bayraktar, A.; Çelebi, B.; Uğuzdoğan, E.; Tuncel, A. Aqueous size exclusion chromatography in semimicro and micro-columns by newly synthesized monodisperse macroporous hydrophilic beads as a stationary phase. *J. Chromatogr. A* **2012,** *1224*, 43-50.

5. Plieva, F. M.; Galaev, I. Y.; Mattiasson, B. Macroporous gels prepared at subzero temperatures as novel materials for chromatography of particulate-containing fluids and cell culture applications. *J. Sep. Sci.* **2007,** *30* (11), 1657-1671.

6. Kim, H.; Lee, J.; Ahn, H.; Kim, O.; Park, M. J. Synthesis of three-dimensionally interconnected sulfur-rich polymers for cathode materials of high-rate lithium-sulfur batteries. *Nat. Commun.* **2015,** *6*, 7278.

7. Noro, S.; Mizutani, J.; Hijikata, Y.; Matsuda, R.; Sato, H.; Kitagawa, S.; Sugimoto, K.; Inubushi, Y.; Kubo, K.; Nakamura, T. Porous coordination polymers with ubiquitous and biocompatible metals and a neutral bridging ligand. *Nat. Commun.* **2015,** *6*, 5851.

8. Reboul, J.; Furukawa, S.; Horike, N.; Tsotsalas, M.; Hirai, K.; Uehara, H.; Kondo, M.; Louvain, N.; Sakata, O.; Kitagawa, S. Mesoscopic architectures of porous coordination polymers fabricated by pseudomorphic replication. *Nat. Mater.* **2012,** *11* (8), 717-723.

9. Svec, F.; Fréchet, J. M. J. New designs of macroporous polymers and supports: From separation to biocatalysis. *Science* **1996,** *273* (5272), 205-211.

10. Gomez, C. G.; Pastrana, G.; Serrano, D.; Zuzek, E.; Villar, M. A.; Strumia, M. C. Macroporous poly(EGDMA-co-HEMA) networks: Morphological characterization from their behaviour in the swelling process. *Polymer* **2012,** *53* (14), 2949-2955.

11. Saba, S. A.; Mousavi, M. P.; Buhlmann, P.; Hillmyer, M. A. Hierarchically Porous Polymer Monoliths by Combining Controlled Macro- and Microphase Separation. *J. Am. Chem. Soc.* **2015,** *137* (28), 8896-8899.

12. Sai, H.; Tan, K. W.; Hur, K.; Asenath-Smith, E.; Hovden, R.; Jiang, Y.; Riccio, M.; Muller, D. A.; Elser, V.; Estroff, L. A.; Gruner, S. M.; Wiesner, U. Hierarchical Porous Polymer Scaffolds from Block Copolymers. *Science* **2013,** *341* (6145), 530-534.

13. Van de Steene, E.; De Clercq, J.; Thybaut, J. W. Ion-exchange resin catalyzed transesterification of ethyl acetate with methanol: Gel versus macroporous resins. *Chem. Eng. J.* **2014,** *242*, 170-179.

14. Cocco, A. P.; Nelson, G. J.; Harris, W. M.; Nakajo, A.; Myles, T. D.; Kiss, A. M.; Lombardo, J. J.; Chiu, W. K. Three-dimensional microstructural imaging methods for energy materials. *PCCP* **2013,** *15* (39), 16377-16407.

15. Müllner, T.; Zankel, A.; Svec, F.; Tallarek, U. Finite-size effects in the 3D reconstruction and morphological analysis of porous polymers. *Mater. Today* **2014,** *17* (8), 404-411.

16. Stoeckel, D.; Kübel, C.; Hormann, K.; Höltzel, A.; Smarsly, B. M.; Tallarek, U. Morphological Analysis of Disordered Macroporous–Mesoporous Solids Based on Physical Reconstruction by Nanoscale Tomography. *Langmuir* **2014,** *30* (30), 9022-9027.

17. Callaghan, P. T. *Translational dynamics and magnetic resonance : principles of pulsed gradient spin echo NMR*; Oxford University Press: Oxford; New York, 2011.

18. Price, W. S. *NMR Studies of Translational Motion*; Cambridge University Press2009.

19. Kimmich, R. *Principles of soft-matter dynamics : basic theories, non-invasive methods, mesoscopic aspects*; Springer: Dordrecht, 2012.

20. Chiavazzo, E.; Fasano, M.; Asinari, P.; Decuzzi, P. Scaling behaviour for the water transport in nanoconfined geometries. *Nat. Commun.* **2014,** *5*, 4565.

21. Solveyra, E. G.; Llave, E. d. l.; Molinero, V.; Soler-Illia, G. J. A. A.; Scherlis, D. A. Structure, Dynamics, and Phase Behavior of Water in TiO2Nanopores. *J. Phys. Chem. C* **2013,** *117* (7), 3330-3342.

22. Nayeri, M.; Aronson, M. T.; Bernin, D.; Chmelka, B. F.; Martinelli, A. Surface effects on the structure and mobility of the ionic liquid C6C1ImTFSI in silica gels. *Soft Matter* **2014,** *10* (30), 5618-5627.

23. Diallo, S. O. Pore-size dependence and characteristics of water diffusion in slitlike micropores. *Phys. Rev. E* **2015,** *92* (1), 012312.

24. Ori, G.; Villemot, F.; Viau, L.; Vioux, A.; Coasne, B. Ionic liquid confined in silica nanopores: molecular dynamics in the isobaric–isothermal ensemble. *Mol. Phys.* **2014,** *112* (9-10), 1350-1361.

25. Brownstein, K. R.; Tarr, C. E. Spin-lattice relaxation in a system governed by diffusion. *J. Magn. Reson.* **1977,** *26* (1), 17-24.

26. Brownstein, K. R.; Tarr, C. E. Importance of classical diffusion in NMR studies of water in biological cells. *Phys. Rev. A: At. Mol. Opt. Phys.* **1979,** *19* (6), 2446-2453.

27. Song, Y. Q.; Ryu, S.; Sen, P. N. Determining multiple length scales in rocks. *Nature* **2000,** *406* (6792), 178-181.

28. Song, Y. Q. Determining Pore Sizes Using an Internal Magnetic Field. *J. Magn. Reson.* **2000,** *143* (2), 397-401.

29. Song, Y. Q.; Sigmund, E. E.; Lisitza, N. V. NMR Pore Size Measurements Using an Internal Magnetic Field in Porous Media. In *NMR Imaging in Chemical Engeneering*, Stapf, S.; Han, S. I., Eds.; Wiley: Weinheim, 2006.

30. Muncaci, S.; Mattea, C.; Stapf, S.; Ardelean, I. Frequency-dependent NMR relaxation of liquids confined inside porous media containing an increased amount of magnetic impurities. *Magn. Reson. Chem.* **2013,** *51* (2), 123-128.

31. Liu, H.; Nogueira d'Eurydice, M.; Obruchkov, S.; Galvosas, P. Determining pore length scales and pore surface relaxivity of rock cores by internal magnetic fields modulation at 2MHz NMR. *J. Magn. Reson.* **2014,** *246*, 110-118.

32. Kimmich, R.; Anoardo, E. Field-cycling NMR relaxometry. *Prog. Nucl. Magn. Reson. Spectrosc.* **2004,** *44* (3-4), 257-320.

33. Stapf, S.; Kimmich, R.; Seitter, R. O. Proton and Deuteron Field-Cycling NMR Relaxometry of Liquids in Porous Glasses: Evidence for Lévy-Walk Statistics. *Phys. Rev. Lett.* **1995,** *75* (15), 2855-2858.

34. Mabry, J. N.; Kastantin, M.; Schwartz, D. K. Capturing Conformation-Dependent Molecule–Surface Interactions When Surface Chemistry Is Heterogeneous. *ACS Nano* **2015,** *9* (7), 7237-7247.

35. Korb, J. P.; Whaley-Hodges, M.; Bryant, R. G. Translational diffusion of liquids at surfaces of microporous materials: Theoretical analysis of field-cycling magnetic relaxation measurements. *Phys. Rev. E* **1997,** *56* (2), 1934-1945.

36. Godefroy, S.; Korb, J. P.; Fleury, M.; Bryant, R. G. Surface nuclear magnetic relaxation and dynamics of water and oil in macroporous media. *Phys. Rev. E* **2001,** *64* (2), 021605.

37. Mitchell, J.; Broche, L. M.; Chandrasekera, T. C.; Lurie, D. J.; Gladden, L. F. Exploring Surface Interactions in Catalysts Using Low-Field Nuclear Magnetic Resonance. *J. Phys. Chem. C* **2013,** *117* (34), 17699-17706.

38. Song, Y. Q. Magnetic resonance of porous media (MRPM): A perspective. *J Magn Reson* **2013,** *229*, 12-24.

39. Kleinberg, R. L.; Kenyon, W. E.; Mitra, P. P. Mechanism of NMR Relaxation of Fluids in Rock. *J. Magn. Reson.* **1994,** *108* (2), 206-214.

40. McDonald, P. J.; Korb, J. P.; Mitchell, J.; Monteilhet, L. Surface relaxation and chemical exchange in hydrating cement pastes: A two-dimensional NMR relaxation study. *Phys. Rev. E* **2005,** *72* (1), 011409.

41. Van Landeghem, M.; d'Espinose de Lacaillerie, J.-B.; Blümich, B.; Korb, J.-P.; Bresson, B. The roles of hydration and evaporation during the drying of a cement paste by localized NMR. *Cem. Concr. Res.* **2013,** *48*, 86-96.

42. Stingaciu, L. R.; Pohlmeier, A.; Blümler, P.; Weihermüller, L.; van Dusschoten, D.; Stapf, S.; Vereecken, H. Characterization of unsaturated porous media by high-field and low-field NMR relaxometry. *Water Resour. Res.* **2009,** *45* (8), W08412.

43. Gomez, C. G.; Alvarez Igarzabal, C. I.; Strumia, M. C. Effect of the crosslinking agent on porous networks formation of hema-based copolymers. *Polymer* **2004,** *45* (18), 6189-6194.

44. Gomez, C. G.; Strumia, M. C. Synthesis and modification of supports with an alkylamine and their use in albumin adsorption. *J. Polym. Sci., Part A: Polym. Chem.* **2008,** *46* (7), 2557-2566.

45. Holz, M.; Heil, S. R.; Sacco, A. Temperature-dependent self-diffusion coefficients of water and six selected molecular liquids for calibration in accurate 1H NMR PFG measurements. *PCCP* **2000,** *2* (20), 4740-4742.

46. Silletta, E. V.; Velasco, M. I.; Gomez, C. G.; Acosta, R. H.; Strumia, M. C.; Monti, G. A. Evaporation kinetics in swollen porous polymeric networks. *Langmuir* **2014,** *30* (14), 4129-4136.

47. Velasco, M. I.; Silletta, E. V.; Gomez, C. G.; Strumia, M. C.; Stapf, S.; Monti, G. A.; Mattea, C.; Acosta, R. H. Spatially Resolved Monitoring of Drying of Hierarchical Porous Organic Networks. *Langmuir* **2016,** *32* (8), 2067-2074.

48. Weber, D.; Mitchell, J.; McGregor, J.; Gladden, L. F. Comparing Strengths of Surface Interactions for Reactants and Solvents in Porous Catalysts Using Two-Dimensional NMR Relaxation Correlations. *J. Phys. Chem. C* **2009,** *113* (16), 6610-6615.

49. Song, Y. Q.; Venkataramanan, L.; Hurlimann, M. D.; Flaum, M.; Frulla, P.; Straley, C. T(1)-T(2) correlation spectra obtained using a fast two-dimensional Laplace inversion. *J. Magn. Reson.* **2002,** *154* (2), 261-268.

50. Giussi, J. M.; Velasco, M. I.; Longo, G. S.; Acosta, R. H.; Azzaroni, O. Unusual temperature-induced swelling of ionizable poly(N-isopropylacrylamide)-based microgels: experimental and theoretical insights into its molecular origin. *Soft Matter* **2015,** *11* (45), 8879-8886.

51. Kowalczuk, J.; Rachocki, A.; Bielejewski, M.; Tritt-Goc, J. Effect of gel matrix confinement on the solvent dynamics in supramolecular gels. *J. Colloid Interface Sci.* **2016,** *472*, 60-68.

52. Tritt-Goc, J.; Rachocki, A.; Bielejewski, M. The solvent dynamics at pore surfaces in molecular gels studied by field-cycling magnetic resonance relaxometry. *Soft Matter* **2014,** *10* (39), 7810-7818.

53. Stapf, S.; Kimmich, R.; Niess, J. Microstructure of porous media and field-cycling nuclear magnetic relaxation spectroscopy. *J. Appl. Phys.* **1994,** *75* (1), 529-537.

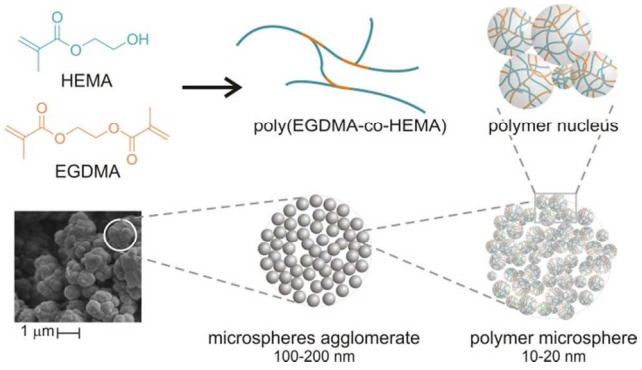

Scheme 1: (color online) Chemical and physical structures for the porous polymeric networks synthesized by a free-radical polymerization of vinyl monomers.

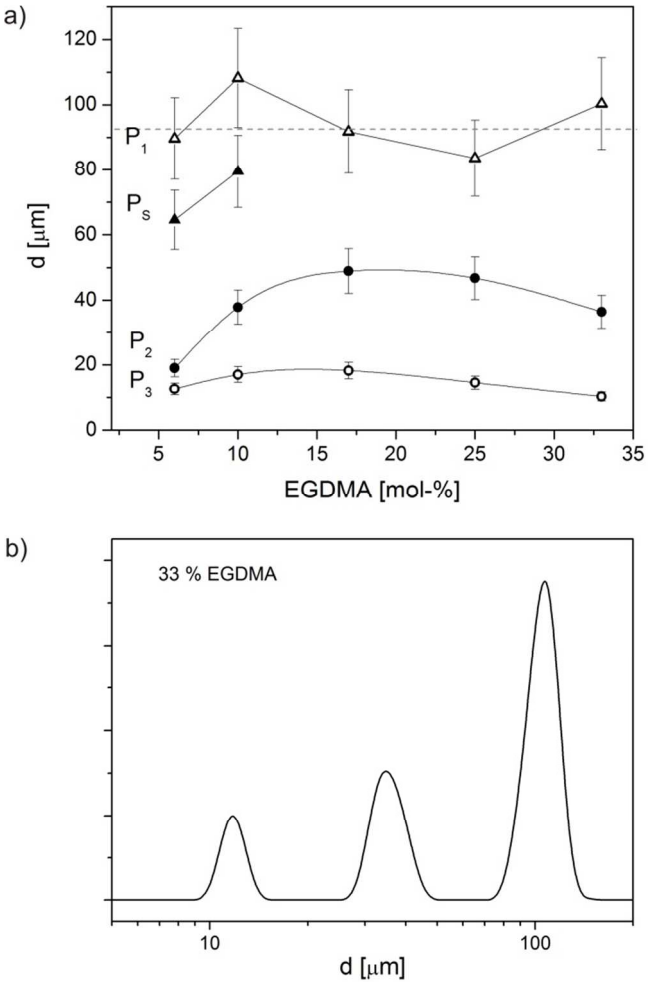

Figure 1. a) Pore diameter of different cavities as a function of the cross-linker percentage obtained with the DDIF sequence. Swelling is detected only as a lower amount of cross-linker is used. The dashed line represents the average pore size of the larger cavities. b) Pore size distribution obtained after an Inverse Laplace Transform of data acquired with the DDIF sequence for networks prepared with 33 mol% of EGDMA.

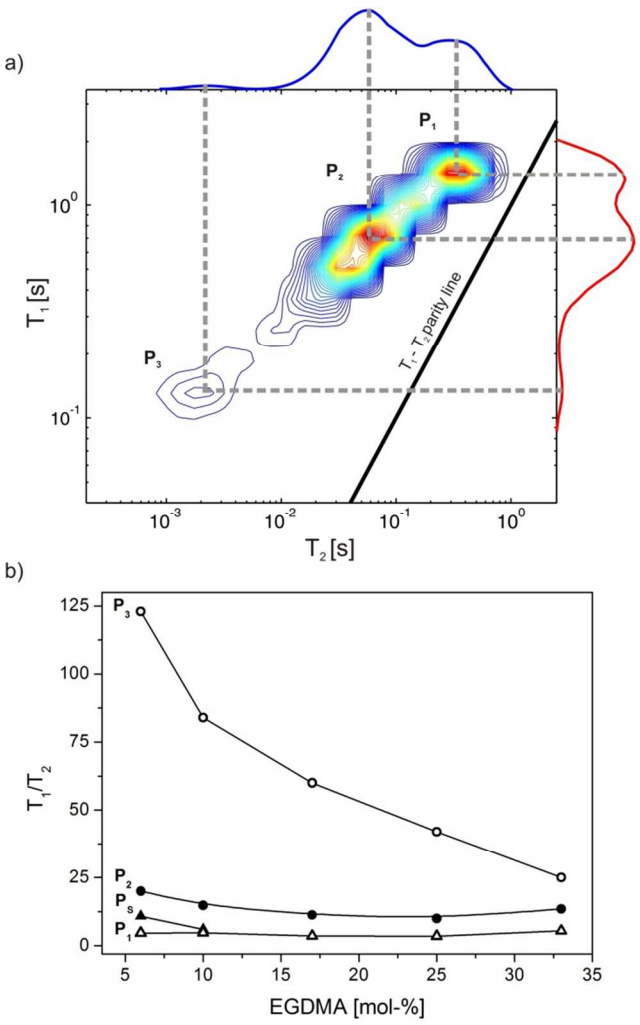

Figure 2. (Color online) a) T_1-T_2 correlation map for a polymer system prepared with a 33 mol % of EGDMA content obtained at 60 MHz. b) T_1/T_2 variations as a function of the cross-linker concentration for water contained in the different cavity sizes.

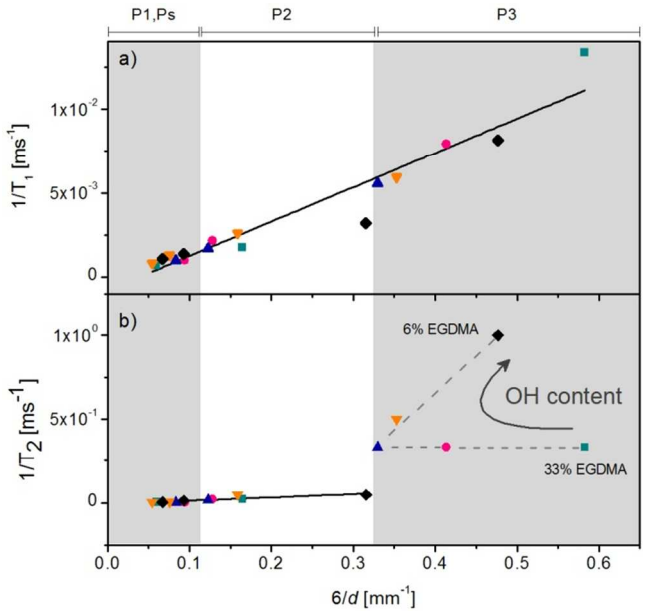

Figure 3. (Color online) a) Longitudinal relaxation rates obtained at 60 MHz for water contained in all cavities of the five samples as a function of the inverse of the pore size. $\rho_1 = (0.020 \pm 0.001)$ mm/s is obtained from the linear fit. b) Transverse relaxation rates as a function of the inverse of the pore size. $\rho_2 = (0.20 \pm 0.04)$ mm/s is obtained from the linear fit only for pores P_1, P_2 and P_s. Relaxation in P_3 is not a surface limited process and changes with the cross-linker content as depicted in the figure.

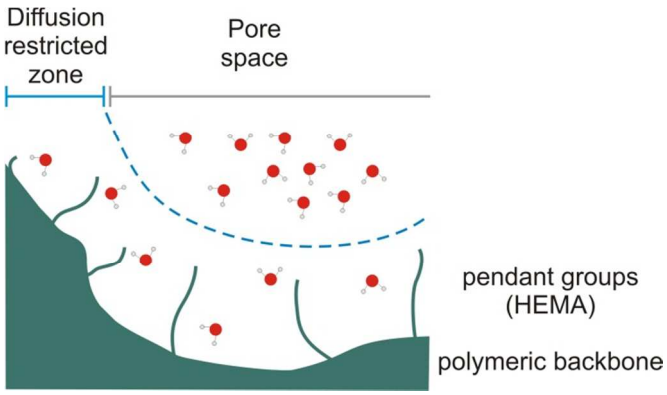

Scheme 2. (Color online) Schematic representation of the different water populations within the sample. Pendant groups determine a zone with restricted diffusion, where the RMTD mechanism is present for the organic polymeric material. Water contained in the pore spaces behaves with the standard restricted diffusion observed for most porous systems.

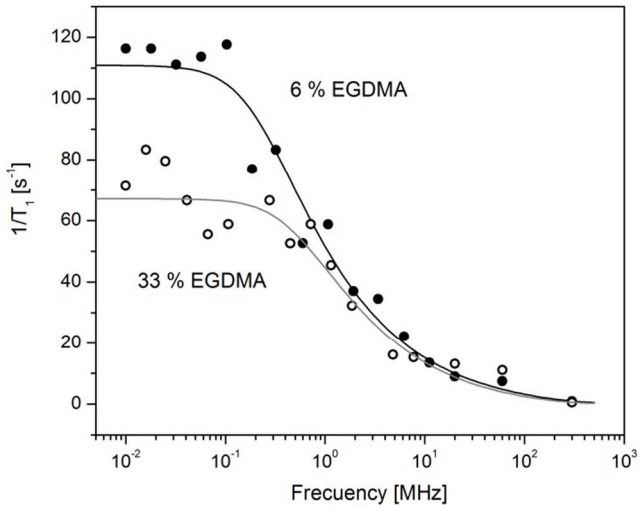

Figure 4. Relaxation dispersion of water confined in smaller cavity sizes, P_3. The solid line corresponds to fittings using a RMTD model.

GRAPHICAL ABSTRACT